Progress In Electromagnetics Research M, Vol. 37, 51–62, 2014

Scattering by a Tilted Strip Buried in a Lossy Half-Space at Oblique Incidence

Mario Lucido*

Abstract—The analysis of the scattering by a tilted perfectly conducting strip buried in a lossy half-space at oblique incidence is formulated as an electric field integral equation (EFIE) in the spectral domain and discretized by means of Galerkin's method with Chebyshev polynomials basis functions weighted with the edge behaviour of the surface current density on the strip. In this way, a convergence of exponential type is achieved. Moreover, a new analytical technique is introduced to rapidly evaluate the slowly converging integrals of the scattering matrix coefficients consisting of algebraic manipulations and a suitable integration procedure in the complex plane.

1. INTRODUCTION

In research areas such as geophysical exploration, remote sensing and target identification, the study of the scattering by buried objects has represented an important issue for several years and even more recently (see [1–3] and the reference therein for an overview).

Indubitably, the most effective technique to analyze the propagation, radiation and scattering by finite objects in layered non-shielded structures consists in formulating the problem as an integral equation in the spatial or the spectral domain, that enables to express the fields as functions of unknowns defined on finite regions, discretized by means of the variational method of moments.

It is well-known that the potential/field Green's functions of a layered medium are expressed in closed form only in the spectral domain and the spatial domain counterparts are represented by slowly converging integrals of Sommerfeld type. Therefore, the efficient evaluation of such kind of integrals is a precondition for rapidly converging spatial domain formulations. Approximate expressions of the spectral domain Green's functions are proposed in [4–11] in order to analytically perform the corresponding Sommerfeld integrals. Despite the remarkable efficiency, the accuracy of such expressions is still object of investigation [5, 12, 13]. On the other hand, appropriate acceleration/extrapolation techniques, change of the integration path and/or suitable quadrature formulas are proposed to speed up the numerical computation of the Sommerfeld integrals [13–19]. Unfortunately, the operation cannot be carried out once because the integrands depend on the frequency and the distance between the source and the field points.

Spectral domain formulations have been largely employed for their simplicity and flexibility to study the propagation, the radiation and the scattering by objects in a layered medium [20–22]. Moreover, when dealing with canonical shape perfectly conducting/dielectric objects with edges in a homogeneous or a layered medium, fast convergence is achieved by means of Galerkin's method with analytically Fourier transformable expansion basis factorizing the behaviour of the fields at the edges [23–44]. Unfortunately, the computation time rapidly increases with the accuracy required for the solution because the elements of the coefficients' matrix are infinite integrals of oscillating functions. Different approaches have been developed in the past and even more recently to overcome this problem. The most popular acceleration technique consists in extracting the asymptotic behaviour from the

Received 15 April 2014, Accepted 16 May 2014, Scheduled 18 June 2014
* Corresponding author: Mario Lucido (lucido@unicas.it).
The author is with the D.I.E.I., Università degli Studi di Cassino e del Lazio Meridionale, Cassino 03043, Italy.

kernels/integrands of the slowly converging integrals and expressing the integrals of the extracted part in closed form [23–27, 29, 32–38, 41]. In the analysis of the propagation in multilayered striplines [39, 42] and the scattering by a rectangular plate in a homogeneous medium [43], the matrix coefficients are rapidly evaluated by using appropriate integration procedures in the complex plane. In order to speed up the analysis of the propagation and the scattering by strips and slots in a layered medium, in [28, 30, 31] the singularity is extracted from the spectral domain Green's function and the corresponding integrals recast in the spatial domain and written in computationally efficient forms. In the analysis of the propagation in single and coupled microstrip lines [40] and of the complex resonances of a rectangular patch in a layered medium [44], a suitable half-space contribution is pulled out of the spectral domain Green's function to obtain exponentially decaying integrands and the slowly converging integrals of the extracted contributions are expressed as combinations of rapidly converging integrals.

The aim of this paper is the accurate and efficient analysis of the scattering by a tilted perfectly conducting strip buried in a lossy half-space. Galerkin's method with Chebyshev polynomials basis functions weighted with the edge behaviour of the surface current density on the strip applied to an EFIE formulation in the spectral domain allows to obtain convergence of exponential type. The generic scattering matrix coefficient is represented as the superposition of two contributions: a rapidly converging scattered contribution due to the inhomogeneity of the medium, and a primary or free space contribution that is rewritten as a combination of proper integrals by means of a new analytical technique consisting of algebraic manipulations and a suitable integration procedure in the complex plane.

In Section 2 the formulation of the problem and the discretization of the integral equations are presented. The new analytical technique to rapidly evaluate the scattering matrix is illustrated in Section 3. Section 4 is devoted to show the accuracy and the efficiency of the presented technique and the conclusions are summarized in Section 5.

2. FORMULATION AND SOLUTION OF THE PROBLEM

In Figure 1 two adjoining half-spaces, of dielectric permittivity $\varepsilon_l = \varepsilon_0\varepsilon_{rl}$, magnetic permeability $\mu_l = \mu_0\mu_{rl}$ and wavenumber $k_l = \omega\sqrt{\varepsilon_l\mu_l} = 2\pi/\lambda\sqrt{\varepsilon_{rl}\mu_{rl}}$ with $l \in \{1, 2\}$, where ε_0 and μ_0 are the dielectric permittivity and the magnetic permeability of the vacuum, ω is the angular frequency and λ is the wavelength in the vacuum, are depicted. A coordinate system (x, y, z) is introduced with the origin on the discontinuity surface and the z axis orthogonal to it. A perfectly conducting strip of dimension $2a$, rotation angle φ, strip axis parallel to the y axis and centred at the point $x = 0$, $z = -d$, is completely immersed in the half-space 2. Moreover, a local coordinate system (x_0, y, z_0) with the origin at the centre of the strip and the z_0 axis orthogonal to it is introduced.

A plane wave of electric field $\underline{E}^{inc}(\underline{r}) = \underline{E}_0 e^{-j\underline{k}\cdot\underline{r}}$, where $\underline{r} = x\hat{x} + y\hat{y} + z\hat{z}$ and $\underline{k} = -k_1(\sin\vartheta_0\cos\varphi_0\hat{x} + \sin\vartheta_0\sin\varphi_0\hat{y} + \cos\vartheta_0\hat{z})$, travelling through the half-space 1 impinges on the discontinuity surface, then, a damped transmitted wave arises in the half-space 2 ($\underline{E}^{tr}(\underline{r}) = \underline{E'}_0 e^{-j\underline{k'}\cdot\underline{r}}$ where $\underline{k'}$ and $\underline{E'}_0$ can be immediately obtained from $\underline{k}$ and $\underline{E}_0$ by means of Snell's law and Fresnel's equations) inducing a current density $\underline{J}(\underline{r})$ in the scatterer.

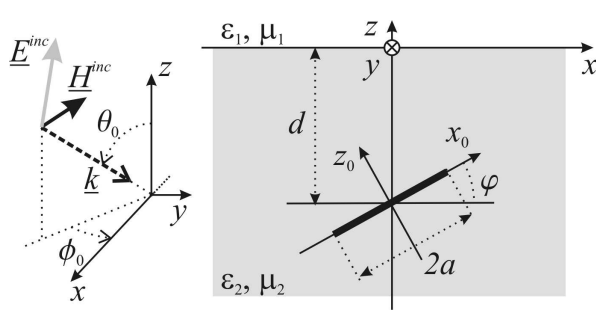

Figure 1. Geometry of the problem.

The vector potential generated by the sources in the half-space 2 is [45, 46]

$$\underline{A}\left(\underline{r}\right)=\int\limits_{-\infty}^{+\infty}\int\limits_{-\infty}^{+\infty}\int\limits_{-\infty}^{+\infty}\underline{\underline{G}}_A\left(\underline{r},\underline{r}'\right)\underline{J}\left(\underline{r}'\right)d\underline{r}', \tag{1}$$

where

$$\underline{\underline{G}}_A\left(\underline{r},\underline{r}'\right)=\frac{\mu_2}{4\pi}\left\{\frac{e^{-jk_2|\underline{r}-\underline{r}'|}}{|\underline{r}-\underline{r}'|}\underline{\underline{I}}+j\frac{1}{2\pi}\int\limits_{-\infty}^{+\infty}\int\limits_{-\infty}^{+\infty}\underline{\underline{\tilde{G}}}\left(u,v\right)e^{-j\left[\underline{g}^-(u,v)\cdot\underline{r}-\underline{g}'^+(u,v)\cdot\underline{r}'\right]}dudv\right\}, \tag{2a}$$

$$\tilde{G}_{xx}\left(u,v\right)=\tilde{G}_{yy}\left(u,v\right)=-D_\mu\left(u,v\right)/R_2\left(u,v\right), \tag{2b}$$

$$\tilde{G}_{xy}\left(u,v\right)=\tilde{G}_{yx}\left(u,v\right)=0, \tag{2c}$$

$$\tilde{G}_{xz}(u,v)\Big/u=\tilde{G}_{yz}(u,v)\Big/v=-\tilde{G}_{zx}(u,v)\Big/u=-\tilde{G}_{zy}(u,v)\Big/v=-[D_\mu(u,v)+D_\varepsilon(u,v)]\big/\left(u^2+v^2\right), \tag{2d}$$

$$\tilde{G}_{zz}\left(u,v\right)=-D_\varepsilon\left(u,v\right)/R_2\left(u,v\right)+R_2\left(u,v\right)\left[D_\mu\left(u,v\right)+D_\varepsilon\left(u,v\right)\right]\big/\left(u^2+v^2\right), \tag{2e}$$

$$D_\eta\left(u,v\right)=\left[\eta_1R_2\left(u,v\right)-\eta_2R_1\left(u,v\right)\right]/\left[\eta_1R_2\left(u,v\right)+\eta_2R_1\left(u,v\right)\right], \tag{2f}$$

$$R_l\left(u,v\right)=\sqrt{k_l^2-u^2-v^2}, \tag{2g}$$

$$\underline{g}^\pm\left(u,v\right)=u\hat{x}+v\hat{y}\pm R_2\left(u,v\right)\hat{z} \tag{2h}$$

with $\eta\in\{\varepsilon,\mu\}$ and $l\in\{1,2\}$.

Since

$$\underline{J}\left(\underline{r}\right)=\left[J_{x_0}\left(x_0\left(x,z\right)\right)\hat{x}_0+J_y\left(x_0\left(x,z\right)\right)\hat{y}\right]e^{-jk_yy}\delta\left(z_0\left(x,z\right)\right), \tag{3}$$

the vector potential can be expressed as follows

$$\underline{A}\left(\underline{r}_0\right)=j\frac{\mu_2}{2}e^{-jk_yy}\left\{-\int\limits_{-\infty}^{+\infty}\frac{e^{-j[ux_0+R_2(u)|z_0|]}}{R_2\left(u\right)}\underline{\tilde{J}}\left(u\right)du+\int\limits_{-\infty}^{+\infty}\underline{\underline{\tilde{G}}}\left(u\right)\underline{\tilde{J}}\left(f_{x_0}^+\left(u\right)\right)e^{-j\left[\underline{f}^-(u)\cdot\underline{r}_0+2R_2(u)d\right]}du\right\} \tag{4}$$

where the functional dependences on $\underline{r}$ and k_y are omitted for the sake of simplicity of notation, $\underline{r}_0=x_0\hat{x}_0+y\hat{y}+z_0\hat{z}_0$, $\underline{\tilde{J}}(\cdot)=\tilde{J}_{x_0}(\cdot)\hat{x}_0+\tilde{J}_y(\cdot)\hat{y}$ is the Fourier transform with respect to the x_0 axis of the surface current density,

$$\underline{f}^\pm\left(u\right)=f_{x_0}^\pm\left(u\right)\hat{x}_0+f_{z_0}^\pm\left(u\right)\hat{z}_0=u\hat{x}\pm R_2\left(u\right)\hat{z}, \tag{5}$$

and the relation [47]

$$\int\limits_{-\infty}^{+\infty}\int\limits_{-\infty}^{+\infty}\frac{e^{-jk_2\sqrt{\left(x_0-x_0'\right)^2+\left(y_0-y_0'\right)^2+z_0^2}}}{\sqrt{\left(x_0-x_0'\right)^2+\left(y_0-y_0'\right)^2+z_0^2}}e^{-j\left(ux_0'+vy_0'\right)}dx_0'dy_0'=-2\pi j\frac{e^{-j[ux_0+vy_0+R_2(u,v)|z_0|]}}{R_2\left(u,v\right)} \tag{6}$$

has been used.

By means of the well-known relation between the vector potential and the electric field, the component of the scattered electric field along the $s\in\{x_0,y\}$ axis can be readily expressed as

$$\begin{aligned}E_s^{sc}\left(\underline{r}_0\right)\;=\;&\frac{e^{-jk_yy}}{2\omega\varepsilon_2}\left\{\int\limits_{-\infty}^{+\infty}\frac{\tilde{G}_{sx0}^{(P)}\left(u\right)\tilde{J}_{x_0}\left(u\right)+\tilde{G}_{sy}^{(P)}\left(u\right)\tilde{J}_y\left(u\right)}{e^{j[ux_0+R_2(u)|z_0|]}}du\right.\\&\left.+\int\limits_{-\infty}^{+\infty}\left[\tilde{G}_{sx0}^{(S)}\left(u\right)\tilde{J}_{x_0}\left(f_{x_0}^+\left(u\right)\right)+\tilde{G}_{sy}^{(S)}\left(u\right)\tilde{J}_y\left(f_{x_0}^+\left(u\right)\right)\right]e^{-j\underline{f}^-(u)\cdot\underline{r}_0}du\right\}\end{aligned} \tag{7}$$

where

$$\underline{\underline{\tilde{G}}}^{(P)}(u) = \frac{1}{R_2(u)}\begin{bmatrix} u^2-k_2^2 & uk_y \\ uk_y & k_y^2-k_2^2 \end{bmatrix}, \tag{8a}$$

$$\tilde{G}_{st}^{(S)}(u) = \frac{U_s^+(u)\,U_t^-(u)\,D_\varepsilon(u) - V_s(u)\,V_t(u)\,D_\mu(u)}{R_2(u)\left(u^2+k_y^2\right)e^{j2R_2(u)d}}, \tag{8b}$$

$$\underline{U}^{\pm}(u) = R_2(u)\left(u\hat{x}+k_y\hat{y}\right) \pm \left(u^2+k_y^2\right)\hat{z}, \tag{8c}$$

$$\underline{V}(u) = k_2\left(k_y\hat{x}-u\hat{y}\right), \tag{8d}$$

superscript P denotes the primary or free space contribution while superscript S denotes the scattered contribution due to the inhomogeneity of the medium.

By imposing the tangential component of the electric field to be vanishing on the strip, an EFIE is obtained

$$\hat{z}_0 \times \underline{E}^{sc}(x_0, y, z_0=0) = -\hat{z}_0 \times \underline{E}^{tr}(x_0, y, z_0=0) \quad \text{for} \quad |x_0| \le a. \tag{9}$$

Generally, no closed form solutions are available, thus, it is necessary to resort to numerical methods. As will be shown in the following, convergence of exponential type can be achieved by expanding the longitudinal and transverse components of the surface current density in series of orthonormal functions consisting of Chebyshev polynomials of first and second kind, respectively, weighted with the edge behaviour of the unknowns, in a Galerkin scheme. Therefore, the Fourier transforms of the current components can be expressed as [48]

$$\tilde{J}_t(u) = \sum_{n=0}^{+\infty} j_{t_n}\xi_{t_n}\frac{J_{n+p_t}(au)}{(au)^{p_t}} \tag{10}$$

with $t \in \{x_0, y\}$, where $p_{x_0}=1$ and $p_y=0$, j_{t_n} is the nth expansion coefficient of the current component along the t axis, $J_\nu(\cdot)$ is the Bessel function of first kind and order ν,

$$\xi_{x_{0n}} = j^n(n+1)\sqrt{\frac{a}{2\pi}}, \tag{11a}$$

$$\xi_{y_n} = j^n\sqrt{\frac{a}{2\pi(1+\delta_{n,0})}}, \tag{11b}$$

are normalization quantities, and $\delta_{n,m}$ is the Kronecker delta.

Therefore, the obtained system of integral equations is reduced to the matrix equation

$$\begin{bmatrix} \mathbf{M}_{x_0x_0} & \mathbf{M}_{x_0y} \\ \mathbf{M}_{yx_0} & \mathbf{M}_{yy} \end{bmatrix}\begin{bmatrix} \mathbf{j}_{x_0} \\ \mathbf{j}_y \end{bmatrix} = \begin{bmatrix} \mathbf{b}_{x_0} \\ \mathbf{b}_y \end{bmatrix} \tag{12}$$

whose coefficients are improper single integrals that can be reviewed as the superposition of a primary contribution and a scattered contribution, i.e.,

$$M_{st_{n,m}} = (-1)^{p_s+p_t}M_{ts_{m,n}} = \xi_{t_n}\xi_{s_m}\left(M_{st_{n,m}}^{(P)} + M_{st_{n,m}}^{(S)}\right), \tag{13a}$$

$$M_{st_{n,m}}^{(P)} = \int_{-\infty}^{+\infty}\tilde{G}_{st}^{(P)}(u)\frac{J_{n+p_t}(au)}{(au)^{p_t}}\frac{J_{m+p_s}(-au)}{(-au)^{p_s}}\,du, \tag{13b}$$

$$M_{st_{n,m}}^{(S)} = \int_{-\infty}^{+\infty}\tilde{G}_{st}^{(S)}(u)\frac{J_{n+p_t}\left(af_{x_0}^+(u)\right)}{\left[af_{x_0}^+(u)\right]^{p_t}}\frac{J_{m+p_s}\left(-af_{x_0}^-(u)\right)}{\left[-af_{x_0}^-(u)\right]^{p_s}}du, \tag{13c}$$

and where the constant terms are

$$b_{s_m} = -2\omega\varepsilon_2\underline{E'}_0\cdot\hat{s}\xi_{s_m}\frac{J_{m+p_s}(-a\underline{k'}\cdot\hat{x}_0)}{(-a\underline{k'}\cdot\hat{x}_0)^{p_s}}e^{j\underline{k'}\cdot\hat{z}d}, \tag{14}$$

with n, m nonnegative integers and $s, t \in \{x_0, y\}$.

3. A NEW ANALYTICAL TECHNIQUE TO EFFICIENTLY EVALUATE THE SCATTERING MATRIX

Starting from the asymptotic behaviour of the Bessel function of first kind [48]

$$J_\nu(w) \overset{|w|\to+\infty}{\sim} \sqrt{\frac{2}{\pi w}} \cos\left(w - \nu\frac{\pi}{2} - \frac{\pi}{4}\right) \quad \text{for} \quad -\pi < \arg(w) < \pi, \tag{15}$$

it is concluded that the integrands of the integrals in (13b) and (13c) are oscillating functions. Despite that, the integral in (13c) is fast convergent for a strip completely immersed in the half-space 2 since the corresponding integrand has an asymptotic decay of the kind $\exp(-2u\alpha)/u^2$, where $\alpha = d - a|\hat{z}\cdot\hat{x}_0| > 0$ is the distance between the edge of the strip closest to the discontinuity surface and the discontinuity surface itself. By comparison, the integrand of the integral in (13b) has a slow asymptotic decay of the kind $1/u^2$. However, such an integral will be expressed in the following as a combination of rapidly converging integrals.

As a first task, by means of the properties [48]

$$2\nu J_\nu(w) = w\left[J_{\nu-1}(w) + J_{\nu+1}(w)\right], \tag{16a}$$

$$J_\nu\left(we^{jq\pi}\right) = e^{jq\nu\pi} J_\nu(w) \text{ with } q \text{ integer}, \tag{16b}$$

it is simple to rewrite (13b) as follows

$$M^{(P)}_{x_0x_{0n,m}} = -\frac{I_{n+1,m+1}}{a^2} - \frac{k_2^2\left(I_{n,m} + I_{n,m+2} + I_{n+2,m} + I_{n+2,m+2}\right)}{4(n+1)(m+1)}, \tag{17a}$$

$$M^{(P)}_{x_0y_{n,m}} = -M^{(P)}_{yx_{0m,n}} = -k_y I_{n,m+1}/a, \tag{17b}$$

$$M^{(P)}_{yy_{n,m}} = \left(k_y^2 - k_2^2\right) I_{n,m}, \tag{17c}$$

where

$$I_{n,m} = \left[(-1)^m + (-1)^n\right] \int_0^{+\infty} J_n(au)\, J_m(au)\, \frac{du}{R_2(u)}, \tag{18}$$

then $I_{n,m} = 0$ for $n+m$ odd and $I_{n,m} = I_{m,n}$ that allow to consider only the cases for $n+m$ even with $n \geq m$.

Now, the functions $f^{(l)}_{n,m}(w) = J_n(aw)H^{(l)}_m(aw)/R_2(w)$ with $l \in \{1,2\}$, where $H^{(l)}_\nu(\cdot) = J_\nu(\cdot) + j(-1)^{l-1}Y_\nu(\cdot)$ is the Hankel function of l-th kind and order ν and $Y_\nu(\cdot)$ is the Bessel function of second kind and order ν, are analytical in the regions of the complex plane $w = u + jv$ delimited by the contours C_l sketched in Figure 2 (where the solid line and the dashed line denote respectively the square-root principal sheet and secondary sheet of the corresponding Riemann surface, and $\bar{k}_2 = \sqrt{k_2^2 - k_y^2}$). Hence,

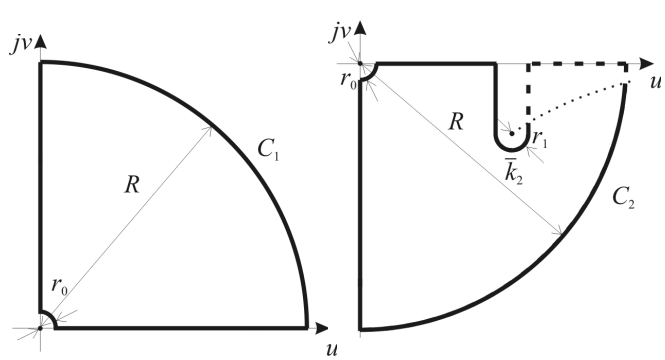

Figure 2. Integration contours in the complex plane.

by means of Cauchy's integral theorem it is possible to write

$$\lim_{\substack{R\to+\infty \\ r_0,r_1\to 0}} \int_{C_l} f_{n,m}^{(l)}(w)\,dw = 0. \tag{19}$$

Remembering (15) and observing that [48]

$$J_\nu(w) \overset{w\to 0}{\sim} (w/2)^\nu/\Gamma(\nu+1) \quad \text{for} \quad \nu \neq -q \text{ with } q \text{ integer}, \tag{20a}$$

$$j\pi(-1)^l H_\nu^{(l)}(w) \overset{w\to 0}{\sim} \begin{cases} 2\ln w & \text{for } \nu = 0 \\ -(2/w)^\nu \Gamma(\nu) & \text{for } \Re\{\nu\} > 0 \end{cases}, \tag{20b}$$

$$H_\nu^{(l)}(w) \overset{|w|\to+\infty}{\sim} \sqrt{\frac{2}{\pi w}} e^{(-1)^{l-1} j(w-\nu\pi/2-\pi/4)} \quad \text{for} \quad -\pi < \arg(w) < \pi, \tag{20c}$$

it can be concluded that the integrands in (19) have at most a logarithmic singularity in $w = 0$ being $n \geq m$, while they decay asymptotically as $1/w^2$ for $0 \leq \arg(w) < \pi$ and $-\pi < \arg(w) \leq 0$ respectively. Therefore, by means of Jordan's lemma, it is simple to rewrite (19), for $l = 1$ and $l = 2$ respectively, as follows

$$\int_0^{+\infty} f_{n,m}^{(1)}(u)\,du = j\int_0^{+\infty} f_{n,m}^{(1)}(jv)\,dv, \tag{21a}$$

$$\int_0^{\bar{k}_2^\Re} f_{n,m}^{(2)}(u)\,du - \int_{\bar{k}_2^\Re}^{+\infty} f_{n,m}^{(2)}(u)\,du = j\int_0^{+\infty} f_{n,m}^{(1)}(jv)\,dv + 2j\int_0^{-\bar{k}_2^\Im} f_{n,m}^{(2)}\left(\bar{k}_2^\Re - jv\right)dv, \tag{21b}$$

the superscripts denoting the real ($\Re$) and the imaginary ($\Im$) part of a complex number, where the (16b) and the relation [48]

$$H_\nu^{(2)}\left(we^{-j\pi}\right) = -e^{j\nu\pi} H_\nu^{(1)}(w) \tag{22}$$

have been used.

The integral in (18) can be simply obtained by taking the half-difference between (21a) and (21b). Hence, (18) can be rewritten as follows

$$I_{n,m} = \left[(-1)^m + (-1)^n\right]\left[\int_0^{\bar{k}_2^\Re} f_{n,m}^{(2)}(u)\,du - j\int_0^{-\bar{k}_2^\Im} f_{n,m}^{(2)}\left(\bar{k}_2^\Re - jv\right)dv\right]. \tag{23}$$

To conclude, the improper integral of an oscillating and slowly decaying function in (13b) has been written as a combination of proper integrals.

4. NUMERICAL RESULTS

The presented technique is very efficient in terms of computation time. Indeed, more than 200 integrals per second are evaluated by using an adaptive Gaussian quadrature routine on a laptop equipped with an Intel Core 2 Duo CPU T9600 2.8 GHz, 3 GB RAM, running Windows XP.

Moreover, the number of integrals to be numerically evaluated is drastically reduced due to the symmetries detailed above. Indeed, despite the overall number of matrix coefficients is $4N^2$ where N is the number of expansion functions used for each component of the surface current density, the number of integrals in (13c) and (18) that have to be computed is respectively $N(2N+1)$ and $N^+(N^-+2)/4$ where $N^\pm = N + 2 \pm \mathrm{mod}(N, 2)$ and $\mathrm{mod}(\cdot,\cdot)$ is the modulus operation.

In order to show the fast convergence of the method, the following normalized truncation error is introduced

$$err(N) = \|\mathbf{j}_{N+1} - \mathbf{j}_N\|/\|\mathbf{j}_N\| \tag{24}$$

where $\|\cdot\|$ is the usual Euclidean norm and $\mathbf{j}_N$ the vector of the expansion coefficients evaluated by using N expansion functions for each component of the surface current density. In Figure 3(a), the normalized truncation error for $\varepsilon_{r1} = \mu_{r1} = \mu_{r2} = 1$, $\varepsilon_{r2} = 4 - j0.5$, $2a = \lambda/2$, λ, 2λ, $d = \lambda$, $\varphi = 30\,\text{deg.}$, when an obliquely incident plane wave with $\underline{E}_0 = (3\sqrt{2}\hat{x} + 4\sqrt{2}\hat{y} - 7\sqrt{3}\hat{z})/\sqrt{197}\,\text{V/m}$ impinges on the discontinuity surface with $\theta_0 = 60\,\text{deg.}$ and $\phi_0 = 45\,\text{deg.}$, is shown. It is clear as the convergence is of exponential type and the number of expansion functions needed to achieve a given accuracy increases more slowly than the dimension of the strip. Similarly, in Figure 3b the normalized truncation error for $2a = \lambda$, $\varphi = 0$, 30, 60, 90 deg. and the same media, buried height and incident plane wave of the previous example is showed. It is clear as the convergence is again of exponential type and substantially independent of the orientation of the strip. For the last example, in Figures 4(a) and 4(b) the components of the surface current density normalized with respect to the tangential component of

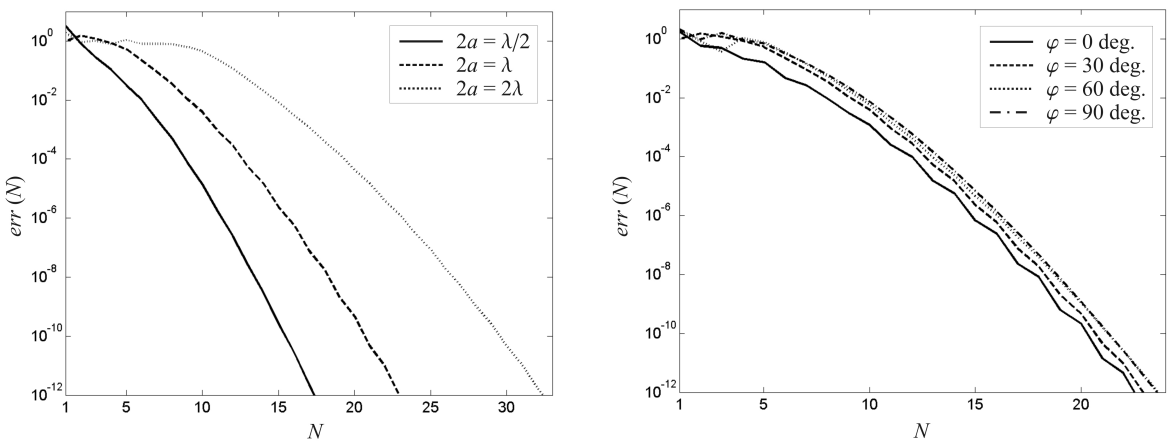

(a) (b)

Figure 3. Normalized truncation error for (a) strips of different dimensions and $\varphi = 30\,\text{deg.}$, and (b) strips of different orientations and $2a = \lambda$. $\varepsilon_{r1} = \mu_{r1} = \mu_{r2} = 1$, $\varepsilon_{r2} = 4 - j0.5$, $d = \lambda$, $\theta_0 = 60\,\text{deg.}$, $\phi_0 = 45\,\text{deg.}$, $\underline{E}_0 = (3\sqrt{2}\hat{x} + 4\sqrt{2}\hat{y} - 7\sqrt{3}\hat{z})/\sqrt{197}\,\text{V/m}$.

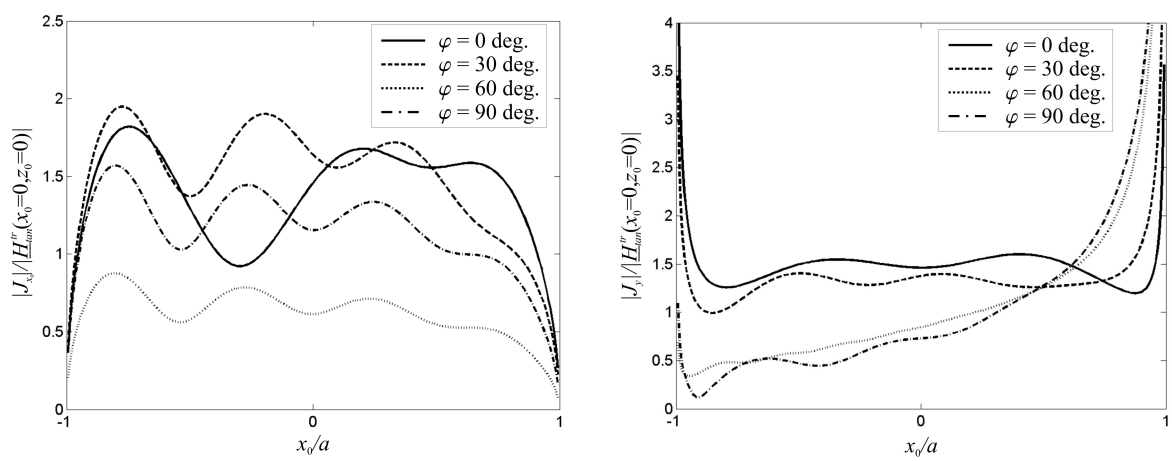

(a) (b)

Figure 4. Normalized components of the surface current density on strips of different orientations. $2a = \lambda$, $\varepsilon_{r1} = \mu_{r1} = \mu_{r2} = 1$, $\varepsilon_{r2} = 4 - j0.5$, $d = \lambda$, $\theta_0 = 60\,\text{deg.}$, $\phi_0 = 45\,\text{deg.}$, $\underline{E}_0 = (3\sqrt{2}\hat{x} + 4\sqrt{2}\hat{y} - 7\sqrt{3}\hat{z})/\sqrt{197}\,\text{V/m}$.

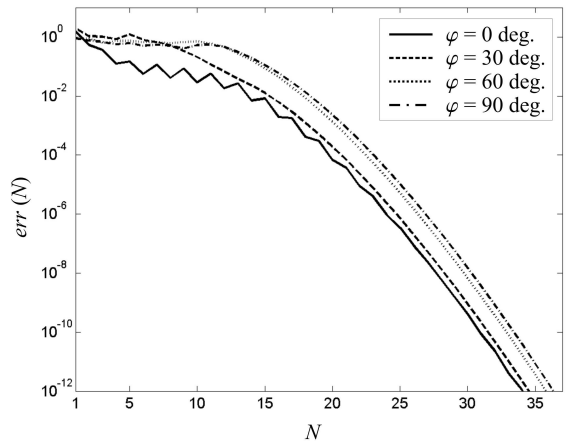

Figure 5. Normalized truncation error for strips of different orientations. $2a = \lambda$, $\varepsilon_{r1} = \mu_{r1} = \mu_{r2} = 1$, $\varepsilon_{r2} = 20 - j3$, $d = \lambda$, $\theta_0 = 60\,\text{deg.}$, $\phi_0 = 45\,\text{deg.}$, $\underline{E}_0 = (3\sqrt{2}\hat{x} + 4\sqrt{2}\hat{y} - 7\sqrt{3}\hat{z})/\sqrt{197}\,\text{V/m}$.

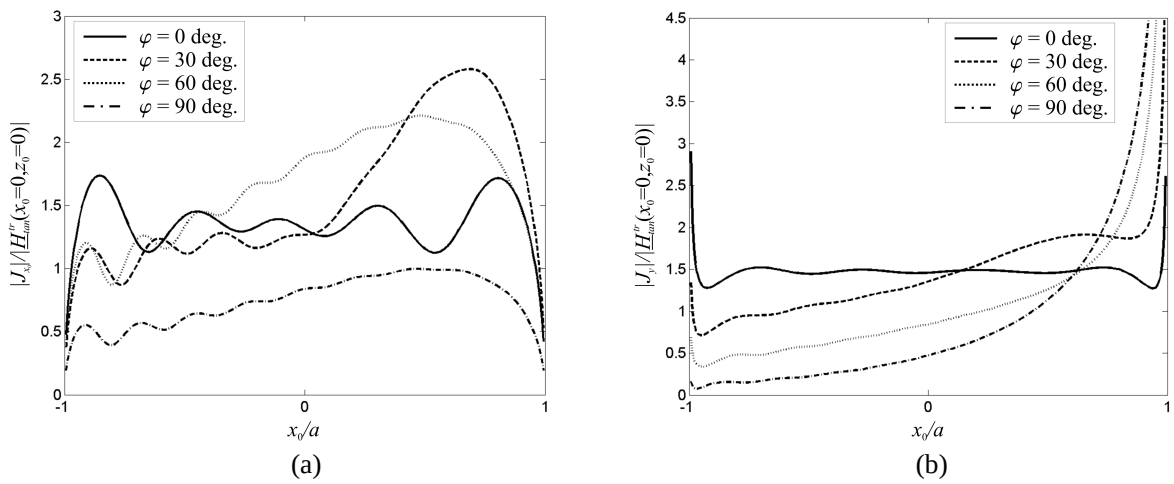

Figure 6. Normalized components of the surface current density on strips of different orientations. $2a = \lambda$, $\varepsilon_{r1} = \mu_{r1} = \mu_{r2} = 1$, $\varepsilon_{r2} = 20 - j3$, $d = \lambda$, $\theta_0 = 60\,\text{deg.}$, $\phi_0 = 45\,\text{deg.}$, $\underline{E}_0 = (3\sqrt{2}\hat{x} + 4\sqrt{2}\hat{y} - 7\sqrt{3}\hat{z})/\sqrt{197}\,\text{V/m}$.

the incident magnetic field evaluated at the centre of the strip, obtained by using 10 expansion functions for each current component in order to achieve a normalized truncation error less than 10^{-2} (henceforth this assumption will be implicitly done) with a computation time of about 1 second, are shown.

In both the previous examples, the dielectric constant of medium 2 is reasonable for a sandy soil with a low soil moisture at X-band microwave frequencies. However, for moderate soil moisture larger dielectric constants must be considered. Just for an example, in Figure 5 the normalized truncation error for $2a = \lambda$, $\varphi = 0, 30, 60, 90\,\text{deg.}$, $\varepsilon_{r2} = 20 - j3$, $\mu_{r2} = 1$ and the same medium 1, buried height and incident plane wave of the previous examples is shown. Once again, the convergence is of exponential type. Compared to the previous example, it is clear that the number of expansion functions needed to achieve a given accuracy increases more slowly than the wavelength in medium 2. For the sake of completeness, in Figures 6(a) and 6(b) the normalized components of the surface current density, obtained by using 19 expansion functions for each current component with a computation time of about 5 seconds, are shown.

To conclude, the correctness of the presented method is verified by comparison with the results

obtained in [49, 50] by means of integral equation formulations discretized with the point-matching method with pulse basis functions.

In Figures 7(a) and 7(b), the normalized surface current density for a strip parallel to the interface ($\varphi = 0\,\text{deg.}$), $\varepsilon_{r1} = \mu_{r1} = \mu_{r2} = 1$, $\varepsilon_{r2} = 4$, $2a = \lambda/2$, $d = 0.1\lambda$, when a TM and a TE plane wave with respect to the y axis impinges on the discontinuity surface with $\theta_0 = 0, 30\,\text{deg.}$ and $\phi_0 = 0\,\text{deg.}$, is reconstructed, by using only 5 expansion functions for each current component with a computation time of 0.25 seconds, and compared with very good agreement with the results presented in [49, 50], respectively.

A very good agreement with the results reported in [49, 50] can be observed even when inclined strips are involved. In Figure 8, the normalized surface current density for the same media and strip dimension of the previous examples, $d = 0.3\lambda$, $\varphi = 30$, $45\,\text{deg.}$, when a TM plane wave normally impinges on the

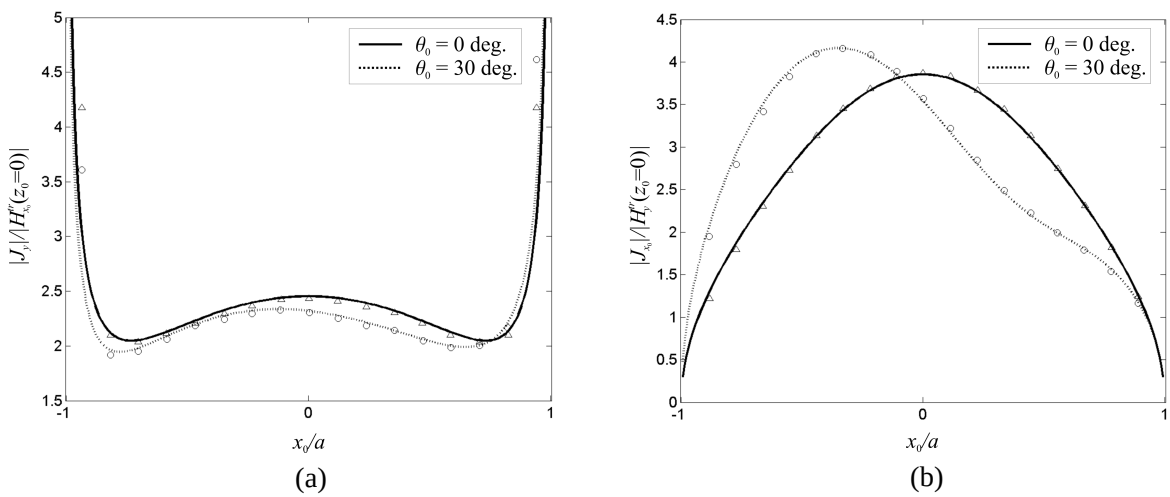

Figure 7. Normalized surface current density for (a) TM incidence and (b) TE incidence. $\varepsilon_{r1} = \mu_{r1} = \mu_{r2} = 1$, $\varepsilon_{r2} = 4$, $2a = \lambda/2$, $d = 0.1\lambda$, $\varphi = 0\,\text{deg.}$, $\phi_0 = 0\,\text{deg.}$ Lines: this method; symbols: data from (a) [49] and (b) [50].

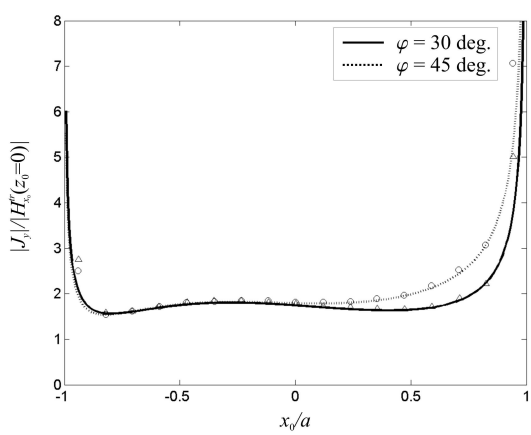

Figure 8. Normalized surface current density for TM incidence. $\varepsilon_{r1} = \mu_{r1} = \mu_{r2} = 1$, $\varepsilon_{r2} = 4$, $2a = \lambda/2$, $d = 0.3\lambda$, $\theta_0 = 0\,\text{deg.}$, $\phi_0 = 0\,\text{deg.}$ Lines: this method; symbols: data from [49].

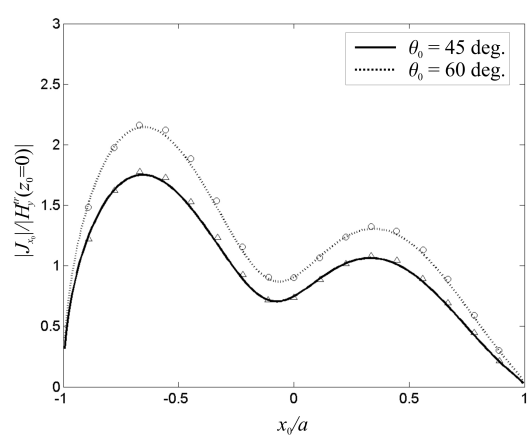

Figure 9. Normalized surface current density for TE incidence. $\varepsilon_{r1} = \mu_{r1} = \mu_{r2} = 1$, $\varepsilon_{r2} = 4$, $2a = \lambda/2$, $d = 0.35\lambda$, $\varphi = 90\,\text{deg.}$, $\phi_0 = 0\,\text{deg.}$ Lines: this method; symbols: data from [50].

discontinuity surface, is accurately reconstructed by using only 6 expansion functions for each current component with a computation time of 0.5 seconds. Similarly, in Figure 9 the normalized surface current density for a strip perpendicular to the interface ($\varphi = 90\,\text{deg.}$), the same media and strip dimension of the previous examples, $d = 0.35\lambda$, when a TE plane wave impinges on the discontinuity surface with $\theta_0 = 45, 60\,\text{deg.}$ and $\phi_0 = 0\,\text{deg.}$, is accurately reconstructed by using only 6 expansion functions for each current component with a computation time of 0.5 seconds.

5. CONCLUSION

In this paper an accurate and efficient analysis of the scattering by a tilted perfectly conducting strip buried in a lossy half-space at oblique incidence has been presented. Future perspectives are the generalization of the method to the analysis of the scattering by polygonal cross-section perfectly conducting and dielectric cylinders buried in a lossy half-space.

ACKNOWLEDGMENT

This work was supported in part by the Italian Ministry of University (MIUR) under a Program for the Development of Research of National Interest (PRIN Grant 20093CJEJ5_002).

REFERENCES

1. Vico, M. D., F. Frezza, L. Pajewski, and G. Schettini, "Scattering by a finite set of perfectly conducting cylinders buried in a dielectric halfspace: A spectral-domain solution," *IEEE Trans. Antennas Propag.*, Vol. 53, No. 2, 719–727, Feb. 2005.
2. Henin, B. H., A. Z. Elsherbeni, and M. H. Al Sharkawy, "Oblique incidence plane wave scattering from an array of circular dielectric cylinders," *Progress In Electromagnetics Research*, Vol. 68, 261–279, 2007.
3. Ahmed, S. and Q. A. Naqvi, "Electromagnetic scattering from a perfect electromagnetic conductor cylinder buried in a dielectric half-space," *Progress In Electromagnetics Research*, Vol. 78, 261–279, 2008.
4. Bernal, J., F. Medina, R. R. Boix, and M. Horno, "Fast full-wave analysis of multistrip transmission lines based on MPIE and complex image theory," *IEEE Trans. Microw. Theory Tech.*, Vol. 48, No. 3, 445–452, Mar. 2000.
5. Rodríguez-Berral, R., F. Mesa, and F. Medina, "Enhanced implementation of the complex images method to study bound and leaky regimes in layered planar printed lines," *IEEE Trans. Microw. Theory Tech.*, Vol. 52, No. 2, 709–720, Feb. 2004.
6. Aksun, M. I. and G. Dural, "Clarification of issues on the closed-form Green's functions in stratified media," *IEEE Trans. Antennas Propag.*, Vol. 53, No. 11, 3644–3653, Nov. 2005.
7. Yuan, M., T. K. Sarkar, and M. Salazar-Palma, "A direct discrete complex image method from the closed-form Green's functions in multilayered media," *IEEE Trans. Microw. Theory Tech.*, Vol. 54, No. 3, 1025–1032, Mar. 2006.
8. Kourkoulos, V. N. and A. C. Cangellaris, "Accurate approximation of Green's functions in planar stratified media in terms of a finite sum of spherical and cylindrical waves," *IEEE Trans. Antennas Propag.*, Vol. 54, No. 5, 1568–1576, May 2006.
9. Boix, R. R., F. Mesa, and F. Medina, "Application of total least squares to the derivation of closed-form Green's functions for planar layered media," *IEEE Trans. Microw. Theory Tech.*, Vol. 55, No. 2, 268–280, 2007.
10. Polimeridis, G., T. V. Yioultsis, and T. D. Tsiboukis, "A robust method for the computation of Green's functions in stratified media," *IEEE Trans. Antennas Propag.*, Vol. 55, No. 7, 1963–1969, 2007.
11. Alparslan, A., M. I. Aksun, and K. A. Michalski, "Closed-form Green's functions in planar layered

media for all ranges and materials," *IEEE Trans. Microw. Theory Tech.*, Vol. 58, No. 3, 602–613, Mar. 2010.

12. Teo, S.-A., S.-T. Chew, and M.-S. Leong, "Error analysis of the discrete complex image method and pole extraction," *IEEE Trans. Microw. Theory Tech.*, Vol. 51, No. 2, 406–413, Feb. 2003.
13. Niciforovic, R. G., A. G. Polimeridis, and J. R. Mosig, "Fast computation of Sommerfeld integral tails via direct integration based on double exponential-type quadrature formulas," *IEEE Trans. Antennas Propag.*, Vol. 59, No. 2, 694–699, Feb. 2011.
14. Dvorak, S. L. and E. F. Kuester, "Numerical computation of 2D sommerfeld integrals — A novel asymptotic extraction technique," *Journal of Computational Physics*, Vol. 98, 217–230, 1992.
15. Michalski, K. A., "Extrapolation methods for Sommerfeld integral tails," *IEEE Trans. Antennas Propag.*, Vol. 46, No. 10, 1405–1418, 1998.
16. Tsang, L., C.-C. Huang, and C. H. Chan, "Surface electric fields and impedance matrix elements of stratified media," *IEEE Trans. Antennas Propag.*, Vol. 48, No. 10, 1533–1543, Oct. 2000.
17. Mosig, J. R. and A. A Melcón, "Green's functions in lossy layered media: Integration along the imaginary axis and asymptotic behavior," *IEEE Trans. Antennas Propag.*, Vol. 51, No. 12, 3200–3208, Dec. 2003.
18. Yuan, M. and T. K. Sarkar, "Computation of the Sommerfeld integral tails using the matrix pencil method," *IEEE Trans. Antennas Propag.*, Vol. 54, No. 4, 1358–1362, 2006.
19. Wu, B. and L. Tsang, "Fast computation of layered medium Green's functions of multilayers and lossy media using fast all-modes method and numerical modified steepest descent path method," *IEEE Trans. Microw. Theory Tech.*, Vol. 56, No. 6, 1446–1454, Jun. 2008.
20. Jansen, R. H., "The spectral domain approach for microwave integrated circuits," *IEEE Trans. Microw. Theory Tech.*, Vol. 33, No. 10, 1043–1056, Oct. 1985.
21. Itoh, T., *Numerical Techniques for Microwave and Millimeter-wave Passive Structures*, Wiley, New York, 1989.
22. Davidson, B. and J. T. Aberle, "An introduction to spectral domain method-of-moments formulations," *IEEE Antennas and Propagat. Mag.*, Vol. 46, No. 3, 11–19, Jun. 2004.
23. Eswaran, K., "On the solutions of a class of dual integral equations occurring in diffraction problems," *Proc. Roy. Soc. London, Ser. A*, 399–427, 1990.
24. Veliev, I. and V. V. Veremey, "Numerical-analytical approach for the solution to thewave scattering by polygonal cylinders and flat strip structures," *Analytical and Numerical Methods in Electromagnetic Wave Theory*, M. Hashimoto, M. Idemen, and O. A. Tretyakov (eds.), Science House, Tokyo, 1993.
25. Park, S. and C. A. Balanis, "Dispersion characteristics of open microstrip lines using closed-form asymptotic extraction," *IEEE Trans. Microw. Theory Tech.*, Vol. 45, No. 3, 458–460, Mar. 1997.
26. Park, S. and C. A. Balanis, "Closed-form asymptotic extraction method for coupled microstrip lines," *IEEE Microw. Guid. Wave Lett.*, Vol. 7, No. 3, 84–86, Mar. 1997.
27. Amari, S., R. Vahldieck, and J. Bornemann, "Using selective asymptotics to accelerate dispersion analysis of microstrip lines," *IEEE Trans. Microw. Theory Tech.*, Vol. 46, No. 7, 1024–1027, Jul. 1998.
28. Tsalamengas, J. L., "Direct singular integral equation methods in scattering and propagation in strip- or slot-loaded structures," *IEEE Trans. Antennas Propag.*, Vol. 46, No. 10, 1560–1570, Oct. 1998.
29. Losada, V., R. R. Boix, and M. Horno, "Resonant modes of circular microstrip patches in multilayered substrates," *IEEE Trans. Microw. Theory Tech.*, Vol. 47, No. 4, 488–498, Apr. 1999.
30. Tsalamengas, J. L., "Exponentially converging direct singular integral-equation methods in the analysis of microslot lines on layered substrates," *IEEE Trans. Microw. Theory Tech.*, Vol. 47, No. 10, 2031–2034, Oct. 1999.
31. Tsalamengas, J. L., "Rapidly converging direct singular integral-equation techniques in the analysis of open microstrip lines on layered substrates," *IEEE Trans. Microw. Theory Tech.*, Vol. 49, No. 3, 555–559, Mar. 2001.

32. Araneo, R., S. Celozzi, G. Panariello, F. Schettino, and L. Verolino, "Analysis of microstrip antennas by means of regularization via Neumann series," *Review of Radio Science 1999–2002*, 111–124, W. R. Stone, Ed., IEEE Press, Wiley Intersci., New York, 2002.
33. Losada, V., R. R. Boix, and F. Medina, "Fast and accurate algorithm for the short-pulse electromagnetic scattering from conducting circular plates buried inside a lossy dispersive half-space," *IEEE Trans. Geosci. Remote Sensing*, Vol. 41, No. 5, 988–997, May 2003.
34. Lucido, M., G. Panariello, and F. Schettino, "Analysis of the electromagnetic scattering by perfectly conducting convex polygonal cylinders," *IEEE Trans. Antennas Propag.*, Vol. 54, 1223–1231, Apr. 2006.
35. Lucido, M., G. Panariello, and F. Schettino, "Electromagnetic scattering by multiple perfectly conducting arbitrary polygonal cylinders," *IEEE Trans. Antennas Propag.*, Vol. 56, No. 2, 425–436, Feb. 2008.
36. Lucido, M., G. Panariello, and F. Schettino, "TE scattering by arbitrarily connected conducting strips," *IEEE Trans. Antennas Propag.*, Vol. 57, No. 7, 2212–2216, Jul. 2009.
37. Lucido, M., G. Panariello, and F. Schettino, "Scattering by polygonal cross-section dielectric cylinders at oblique incidence," *IEEE Trans. Antennas Propag.*, Vol. 58, No. 2, 540–551, Feb. 2010.
38. Coluccini, G., M. Lucido, and G. Panariello, "TM scattering by perfectly conducting polygonal cross-section cylinders: A new surface current density expansion retaining up to the second-order edge behavior," *IEEE Trans. Antennas Propag.*, Vol. 60, No. 1, 407–412, Jan. 2012.
39. Lucido, M., "An analytical technique to fast evaluate mutual coupling integrals in spectral domain analysis of multilayered coplanar coupled striplines," *Microw. Opt. Technol. Lett.*, Vol. 54, 1035–1039, Apr. 2012.
40. Lucido, M., "A new high-efficient spectral-domain analysis of single and multiple coupled microstrip lines in planarly layered media," *IEEE Trans. Microw. Theory Tech.*, Vol. 60, No. 7, 2025–2034, Jul. 2012.
41. Coluccini, G., M. Lucido, and G. Panariello, "Spectral domain analysis of open single and coupled microstrip lines with polygonal cross-section in bound and leaky regimes," *IEEE Trans. Microw. Theory Tech.*, Vol. 61, No. 2, 736–745, Feb. 2013.
42. Lucido, M., "An efficient evaluation of the self-contribution integrals in the spectral-domain analysis of multilayered striplines," *IEEE Antennas Wireless Propag. Lett.*, Vol. 12, 360–363, Mar. 2013.
43. Coluccini, G. and M. Lucido, "A new high efficient analysis of the scattering by a perfectly conducting rectangular plate," *IEEE Trans. Antennas Propag.*, Vol. 61, No. 5, 2615–2622, May 2013.
44. Lucido, M., "Complex resonances of a rectangular patch in a multilayered medium: A new accurate and efficient analytical technique," *Progress In Electromagnetics Research*, Vol. 145, 123–132, 2014.
45. Chew, W. C., *Waves and Fields in Inhomogeneous Media*, IEEE Press, New York, 1995.
46. Chew, W. C. and S. Y. Chen, "Response of a point source embedded in a layered medium," *IEEE Antennas Wireless Propag. Lett.*, Vol. 2, 254–258, 2003.
47. Scott, R., *The Spectral Domain Method in Electromagnetics*, Artech House, Norwood, MA, 1989.
48. Abramowitz, M. and I.A. Stegun, *Handbook of Mathematical Functions*, Verlag Harri Deutsch, 1984.
49. Butler, M., X.-B. Xu, and A. W. Glisson, "Current induced on a conducting cylinder located near the planar interface between two semi-infinite half-spaces," *IEEE Trans. Antennas Propag.*, Vol. 33, No. 6, 616–624, Jun. 1985.
50. Xu, X.-B. and C. M. Butler, "Current induced by TE excitation on a conducting cylinder located near the planar interface between two semi-infinite half-spaces," *IEEE Trans. Antennas Propag.*, Vol. 34, No. 7, 880–890, Jul. 1986.